

Lawrence Berkeley National Laboratory

Recent Work

Title

Ultrafast Dynamics of Excited Electronic States in Nitrobenzene Measured by Ultrafast Transient Polarization Spectroscopy.

Permalink

<https://escholarship.org/uc/item/1cr8q5kw>

Journal

The journal of physical chemistry. A, 124(13)

ISSN

1089-5639

Authors

Thurston, Richard
Brister, Matthew M
Tan, Liang Z
[et al.](#)

Publication Date

2020-04-01

DOI

10.1021/acs.jpca.0c01943

Supplemental Material

<https://escholarship.org/uc/item/1cr8q5kw#supplemental>

Peer reviewed

Ultrafast Dynamics of Excited Electronic States in Nitrobenzene Measured by Ultrafast Transient Polarization Spectroscopy

Richard Thurston,[†] Matthew M. Brister,[†] Liang Z. Tan,[‡] Elio G. Champenois,^{†,¶}
Said Bakhti,[†] Pavan Muddukrishna,[†] Thorsten Weber,[†] Ali Belkacem,[†] Daniel S.
Slaughter,^{*,†} and Niranjana Shivaram^{*,†,§}

[†]*Chemical Sciences Division, Lawrence Berkeley National Laboratory, Berkeley, CA 94720
USA*

[‡]*Molecular Foundry, Lawrence Berkeley National Laboratory, Berkeley, CA 94720 USA*

[¶]*Graduate Group in Applied Science and Technology, University of California, Berkeley,
CA 94720*

[§]*Current address: Department of Physics and Astronomy, Purdue University, West
Lafayette, IN 47907 USA*

E-mail: dsslaughter@lbl.gov; niranjan@purdue.edu

Abstract

We investigate ultrafast dynamics of the lowest singlet excited electronic state in liquid nitrobenzene using Ultrafast Transient Polarization Spectroscopy, extending the well known technique of optical Kerr effect spectroscopy to excited electronic states. The third-order nonlinear response of the excited molecular ensemble is measured using two femtosecond pulses following a third femtosecond pulse that populates the S_1 excited state. By measuring this response, which is highly sensitive to details of the excited state character and structure, as a function of time delays between the three pulses involved, we extract the dephasing time of the wave-packet on the excited state. The dephasing time, measured as a function of time-delay after pump excitation, shows oscillations indicating oscillatory wave-packet dynamics on the excited state. From the experimental measurements and supporting theoretical calculations, we deduce that the wave-packet completely leaves the S_1 state potential energy surface after three traversals of the inter-system crossing between the singlet S_1 and triplet T_2 states.

Introduction

Ultrafast dynamics on excited electronic potential energy surfaces in molecules can occur on time scales ranging from a few femtoseconds to hundreds of picoseconds. In polyatomic molecules with multiple degrees of freedom, conical intersections exist between different electronic potential energy surfaces that allow efficient redistribution of population between different electronic states and, in some cases, rapid nonradiative relaxation to the ground electronic state.¹ Such dynamics may be probed by femtosecond time-resolved techniques such as time-resolved photoelectron spectroscopy^{2,3} or transient absorption spectroscopy,⁴ both of which can measure the evolution of electronic binding energies on ultrafast timescales. In transient absorption spectroscopy, a small fraction of the probe light is absorbed by a sample that interacts with a pump pulse. Probe photons not absorbed by the pumped molecules constitute a background that must be subtracted to determine the change in

absorption, which can limit sensitivity, particularly when performed with light sources having limited spectral or intensity stability such as ultrashort pulsed extreme ultraviolet or X-ray light sources.

Nonlinear spectroscopies employing four-wave mixing (FWM) techniques such as Degenerate Four-Wave Mixing⁵⁻⁷ or optical Kerr effect (OKE),⁸⁻¹⁰ on the other hand, can be background-free. These FWM methods provide information on excited state dynamics when the pulses involved are resonant with the state of interest. However, they rely on electronic coherence between the ground and excited states that is usually established by the first pulse in the FWM sequence. This electronic coherence may not persist long enough to allow the excited state dynamics to be followed completely, due to decoherence caused by inter-nuclear motion. The non-linear response of the excited molecule potentially provides a more comprehensive measure of excited state dynamics. This can be achieved by introducing an additional excitation pulse that first populates specific electronic states, which are probed by four-wave mixing. In this work we demonstrate that a nonlinear probe, combined with an electronic excitation pump pulse, can probe dynamics near inter-system crossing (ISC) geometries or conical intersections (CI), where the potential energy surfaces are degenerate.

The electronic excited states of nitrobenzene have been previously investigated experimentally¹¹⁻¹⁴ and theoretically.¹⁵⁻¹⁸ Transient grating spectroscopy experiments^{13,19} measured three different time scales for dynamics after excitation of the singlet S_1 state. The shortest time-scale measured in that study was ~ 100 fs for the internal relaxation dynamics on the $S_1(n\pi^*)$ state before the wave-packet reaches an ISC with the triplet $T_2(\pi\pi^*)$ state. A more recent theoretical study¹⁸ provides two explanations for the rapid decay times in the transient grating experiments.¹³ The ~ 100 fs lifetime is attributed to either the time taken to reach the S_1/T_2 ISC, or the time to reach a CI between the excited S_1 and ground S_0 electronic states. A very high (0.8) quantum yield¹⁹ of the triplet T_2 state is consistent with the calculated strong coupling between S_1 and T_2 states¹⁸ at the ISC. This strong coupling indicates that the ISC between S_1 and T_2 may be partially responsible for the ~ 100 fs decay

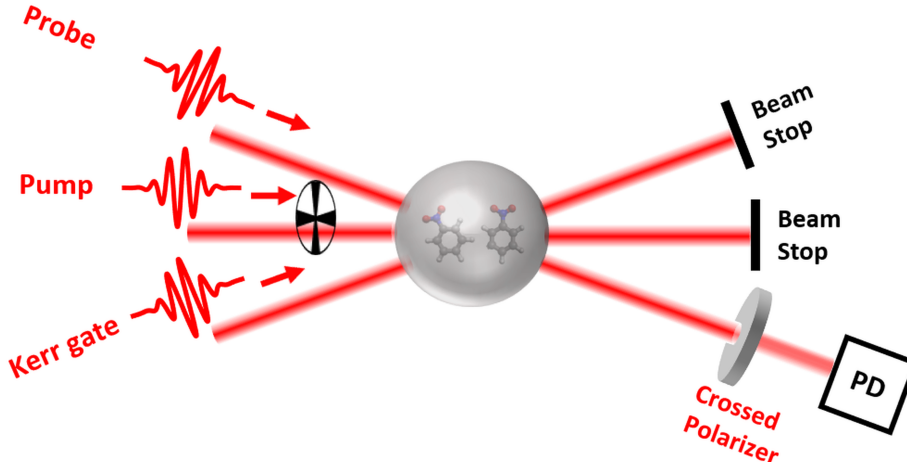


Figure 1: A schematic of the UTPS experimental setup. The pump, probe, and Kerr gate pulses are spatially and temporally overlapped at the nitrobenzene target. The polarization of the probe is fixed at 45° with respect to the Kerr gate polarization. The pump pulse polarization can be varied using a half-wave plate. After interacting with the target, the probe pulse goes through an ultra-high contrast crossed polarizer and is focused onto a photo-diode (PD). The Kerr gate and the pump beam are blocked by a beam stop. Lenses used to focus the beam onto photo-diodes are not shown.

component, for excitation to S_1 , that was measured in the transient grating experiments.¹³ Here, we measure the dephasing time of the excited wave-packet as a function of time delay after excitation. From this measurement we deduce that the wave-packet exhibits oscillatory dynamics on the S_1 state, with a period of ~ 177 fs, and completely leaves the S_1 state after three traversals of the ISC.

We measure the third-order non-linear response of liquid nitrobenzene molecules that are first excited to the S_1 electronic state by two-photon absorption of a pump pulse. In addition to the pump pulse, we use two pulses that together form a probing pulse pair. We use the OKE to measure the non-linear response of the pump-excited molecules. We call this new technique Ultrafast Transient Polarization Spectroscopy (UTPS). This scheme is similar to the method of pump-Degenerate Four-Wave Mixing (pump-DFWM)²⁰ but offers several advantages. Firstly, UTPS uses only two pulses in the probing sequence as opposed to three in pump-DFWM. Secondly, the simple phase matching conditions of the OKE sends the signal along the same direction as one of the probing pulses, which simplifies the experimental

set-up. Finally, since the signal is emitted along the direction of either probing pulse, two signals can be measured on two detectors simultaneously to obtain additional information in one time delay-scanning experiment. Further details and examples of these different signals will be published elsewhere. The relative simplicity of this scheme to measure excited state third-order non-linear response allows for the extension of the pump wavelength to vacuum-ultraviolet, extreme-ultraviolet and even soft X-ray regimes by using a high-order harmonic generation or a free electron laser source.

This paper is organized as follows. After a description of the relevant technical details of the present experiments and calculations, we present new UTPS results on excited nitrobenzene. The analysis of the signal decay times between the Kerr gate and probe pulses reveals information on the excited wavepacket dephasing behavior. We examine the dephasing dependence on the probe delay, relative to the excitation pump pulse, making comparisons with previous electronic structure calculations of the low lying excited states in nitrobenzene and the present calculations of the effective third-order susceptibility. We conclude that the measured dephasing times are found to be consistent with a time-dependent nonlinear response to the nonradiative relaxation dynamics of excited nitrobenzene.

Experimental and Theoretical Methods

The experimental setup is shown in Figure 1. Near-infrared pulses with a central wavelength of 780 nm and pulse duration of ~ 45 fs are first split into two beams using a 50/50 beam-splitter. One arm forms the pump beam and the other is split again with a second 50/50 beam-splitter into two arms creating beams for probe and Kerr gate pulses. Separate optical delay stages generate the two different time delays. One is the time delay (T) between the pump and probe pulses. The other time delay (τ) is the delay between the probe and Kerr gate pulses. When T is varied at fixed τ , the delay of both probe and Kerr gate pulses with respect to the pump varies at the same time. All three pulses intersect at the sample target

in a small angle non-collinear geometry. The time-smearing introduced by the crossing angle is small compared to each pulse duration. The spatial and temporal overlap between the three femtosecond pulses is found pair-wise, using second harmonic generation in a beta barium borate crystal. The experimental target is contained in a thin Spectrosil quartz cuvette with a wall thickness of 1 mm and a sample path length of 1 mm, filled with liquid nitrobenzene. Liquid nitrobenzene was obtained from Sigma Aldrich (> 99% purity) and was used as received at room temperature. After passing through the sample, the pump and Kerr gate beams are blocked by a beam stop. The signal is separated from the collinear probe beam using an ultra-high contrast polarizer (extinction ratio > 10^6), after which the signal is focused onto a photo-diode using a lens. The intensity of the pump pulse is $\sim 5 \times 10^{11}$ W/cm² and the intensity of the probe and Kerr gate pulses are $\sim 2 \times 10^{11}$ W/cm². The pump beam is modulated using a chopper wheel, which provides a reference for a lock-in amplifier used for the measurement.

The UTPS polarization signal measured in this optical homodyne configuration is related to the effective $\chi^{(3)}$,^{9,21} henceforth denoted by $\chi_{eff}^{(3)}$, as a function of the time delays between the pulses. The measured raw UTPS signal can be written as

$$\begin{aligned}
I_{raw}(\tau, T) &= \int \left| E_{sig}(\omega, \tau, T) \right|^2 d\omega \\
&= \int \left| \left[\chi_{eff,g}^{(3)}(\omega, \tau) |E_{Kerr}(\omega)|^2 E_{probe}(\omega) + \chi_{eff,g}^{(3)}(\omega, T) |E_{pump}(\omega)|^2 E_{probe}(\omega) \right. \right. \\
&\quad \left. \left. + \chi_{eff,ex}^{(3)}(\omega, \tau, T) |E_{Kerr}(\omega)|^2 E_{probe}(\omega) \right] \right|^2 d\omega \quad (1)
\end{aligned}$$

where $\chi_{eff,g}^{(3)}$ and $\chi_{eff,ex}^{(3)}$ are the effective third-order susceptibilities, due to the ground-state and excited-state populations, respectively. E_{sig} , E_{probe} , E_{Kerr} , and E_{pump} are the corresponding spectral amplitudes of the electric-fields of the signal along the probe direction and the probe, Kerr gate and pump pulses respectively. All constants have been absorbed into the susceptibilities. The terms involving all three spectral amplitudes of the pump,

probe and Kerr gate pulses are not included, because the signal from such an interaction will not reach the detector due to phase matching constraints. The weak intensity of the Kerr gate and probe pulses are too low to drive higher-order processes such as six-wave mixing.

Equation 1 can be expanded as:

$$\begin{aligned}
I_{raw}(\tau, T) &= \int \left| E_{sig}(\omega, \tau, T) \right|^2 d\omega \\
&= \int \left[|\chi_{eff,g}^{(3)}(\omega, \tau)|^2 |E_{Kerr}(\omega)|^4 |E_{probe}(\omega)|^2 + |\chi_{eff,g}^{(3)}(\omega, T)|^2 |E_{pump}(\omega)|^4 |E_{probe}(\omega)|^2 \right. \\
&\quad + |\chi_{eff,ex}^{(3)}(\omega, \tau, T)|^2 |E_{Kerr}(\omega)|^4 |E_{probe}(\omega)|^2 + \chi_{eff,g}^{(3)}(\omega, \tau) \chi_{eff,g}^{(3)}(\omega, T)^* |E_{Kerr}(\omega)|^2 |E_{pump}(\omega)|^2 |E_{probe}(\omega)|^2 \\
&\quad + \chi_{eff,g}^{(3)}(\omega, \tau) \chi_{eff,ex}^{(3)}(\omega, \tau, T)^* |E_{Kerr}(\omega)|^4 |E_{probe}(\omega)|^2 \\
&\quad \left. + \chi_{eff,g}^{(3)}(\omega, T) \chi_{eff,ex}^{(3)}(\omega, \tau, T)^* |E_{pump}(\omega)|^2 |E_{Kerr}(\omega)|^2 |E_{probe}(\omega)|^2 + c.c \right] d\omega
\end{aligned} \tag{2}$$

where $c.c$ represents complex conjugate. The time delay dependence of the spectral amplitudes appears as phase terms that disappear upon simplification and hence are not included here. Since we perform a lock-in measurement that measures signal only when the pump beam is present, the first term on the right hand side in equation 2 does not contribute. We also subtract the signal measured when the Kerr gate pulse is blocked. This removes the second term in equation 2. After these subtractions and further simplification, the processed signal I_{proc} can be written as,

$$\begin{aligned}
I_{proc}(\tau, T) &= a_1 |\chi_{eff,ex}^{(3)}(\tau, T)|^2 + a_2 \chi_{eff,g}^{(3)}(\tau) \chi_{eff,g}^{(3)}(T)^* + a_1 \chi_{eff,g}^{(3)}(\tau) \chi_{eff,ex}^{(3)}(\tau, T)^* \\
&\quad + a_2 \chi_{eff,g}^{(3)}(T) \chi_{eff,ex}^{(3)}(\tau, T)^* + c.c \tag{3}
\end{aligned}$$

where we have assumed that the third-order susceptibilities are constant within the bandwidth of our laser pulses. a_1 and a_2 are constants obtained after integration of the spectral amplitudes over frequency. We note that $|E_{pump}|^2$ is larger than $|E_{probe}|^2$ and $|E_{Kerr}|^2$ by a factor of ~ 3 in our experiment and the third-order susceptibilities $\chi_{eff}^{(3)}$ are proportional to

the number of molecules in the focal volume. From measurements of the pump absorption (see Figure 2 (b)), we estimate that the number of excited molecules is approximately 10 times smaller than the number of molecules in the ground electronic state that can interact with the Kerr gate and probe photons. This allows us to drop terms containing a_1 and write equation 3 as

$$I_{proc}(\tau, T) \approx a_2 \chi_{eff,g}^{(3)}(\tau) \chi_{eff,g}^{(3)}(T)^* + a_2 \chi_{eff,g}^{(3)}(T) \chi_{eff,ex}^{(3)}(\tau, T)^* + c.c \quad (4)$$

Here, we focus on obtaining information about excited state dynamics through the T dependent dephasing times along the τ axis which has contributions only from $\chi_{eff,ex}^{(3)}(\tau, T)$. The pump intensities used here induce two-photon absorption (see Figure 2 (b)) and other pump interactions, such as spontaneous Raman scattering or stimulated Raman scattering are not expected to contribute significantly to the measured signal. Intermolecular dynamics, such as the response of the unexcited nitrobenzene solvent to an excited nitrobenzene molecule, may contribute to the signal.^{22,23}

To understand the dependence of $\chi_{eff,g}^{(3)}$ and $\chi_{eff,ex}^{(3)}$ on molecular geometry, we perform third-order susceptibility calculations using the sum-over-states method.^{24,25} Molecular orbital energies and dipole matrix elements used in this sum were calculated within density functional theory, with the B3LYP exchange correlation functional, norm-conserving pseudopotentials, and using the Quantum Espresso code.²⁶ Molecular geometries for these calculations were taken from Ref.¹⁸ The sum-over-states was performed as a sum over molecular orbitals, by assuming a single Slater determinant, and using a total of 82 molecular orbitals. $\chi_{eff}^{(3)}$ calculations were performed for the electronic ground state and the excited S_1 and T_2 states. For the excited states, the Slater determinant with the highest weight was used, which was HOMO-3→LUMO for S_1 and HOMO-2→LUMO for T_2 .¹⁷ To account for the

random orientation of molecules in isotropic media, we take $\chi_{eff}^{(3)} = \chi_{xyyx}^{(3)} + \chi_{xyxy}^{(3)}$.^{27,28}

Results and Discussion

The UTPS signal along the probe direction, as a function of the time delays τ and T , after subtraction of the ground state-only contributions, is shown in Figure 2 (a). The data were obtained by acquiring the UTPS signal over 1000 laser shots at each pair of delays and by scanning the delays in a randomized sequence. This scanning procedure was repeated 24 times and the data were then averaged. The zero of time delays τ and T were found by measuring a cross-correlation signal in a second harmonic generation crystal. The time-zero values are accurate to within 10 fs. Figure 2 (b) shows the pump intensity absorbed by the sample, as a function of the incident intensity, which follows a quadratic trend (straight line with gradient of 2 on the log-log plot). The quadratic dependence of the absorbed pump intensity on the incident pump intensity is consistent with two-photon absorption to the S_1 excited electronic state,¹³ previously measured by photoabsorption spectroscopy²⁹ in a band spanning 300~400 nm. Figure 2 (c) indicates the polarization angles of the three pulses and the time delays between them. The polarization angle of the probe is 45° with respect to the polarization of the Kerr gate to achieve a strong OKE interaction. The pump polarization defines the coordinate system, and it is expected that the dipole moment of the molecule will be aligned along the pump polarization for two-photon excitation to S_1 . By repeating the measurement for different Kerr gate polarization angles (with probe always 45° to the Kerr gate), relative to the pump polarization, the UTPS signal will depend on different tensor elements of excited state $\chi^{(3)}$. It is perhaps not surprising that we measure a stronger UTPS signal when the Kerr gate polarization is parallel to the pump polarization. This may be due to the expected alignment of the pump-induced dipole moment of excited nitrobenzene molecules in the pump polarization direction. The UTPS signal is seen to vary with both time delays τ and T . As discussed below, the decay of the signal along the T axis is due to

dynamics on the excited state and along the τ axis is due to dephasing on the excited state. The signal is significant at negative values of τ and T (until ≈ -100 fs) due to the temporal overlap of the pulses, each having a ~ 45 fs pulse duration.

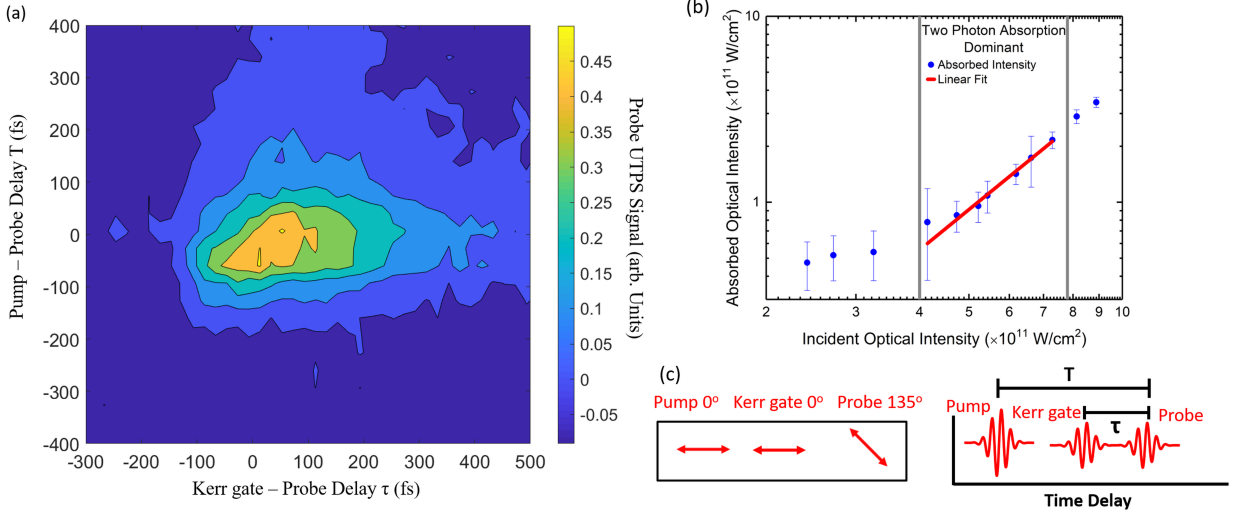


Figure 2: (a) The S_1 excited state UTPS signal measured for liquid nitrobenzene, using near infrared femtosecond pulses, measured along the probe direction. Any two pulse interaction contributions have been subtracted. (b) A plot of the absorbed intensity (blue filled circles) as a function of incident intensity of the pump pulse on a log-log scale and linear fit (solid red line) of the data in the region enclosed by the grey bars. The error bars represent one standard deviation. We obtain a slope of 2.1 ± 0.17 from the fit, consistent with a two-photon process. (c) The polarization angles and time delays between the pump, probe, and Kerr gate. When T is varied at fixed τ , both Kerr gate and probe pulses are delayed with respect to the pump. When τ is varied at fixed T , the probe is delayed with respect to the Kerr gate. At positive T values, the probe and Kerr gate arrive after the pump. At positive τ values the probe arrives after the Kerr gate pulse.

Following Equation 4, the most significant nonlinear response term that is a function of both τ and T is $\chi_{eff,ex}^{(3)}$. In order to extract excited state information, we fit lineouts of the probe UTPS signal, taken at different values of T , with the following equation, which is a convolution of a Gaussian function with an exponential decay. A step function is also included to model any long decay dynamics that does not return the signal back to zero in the range of delay shown here:

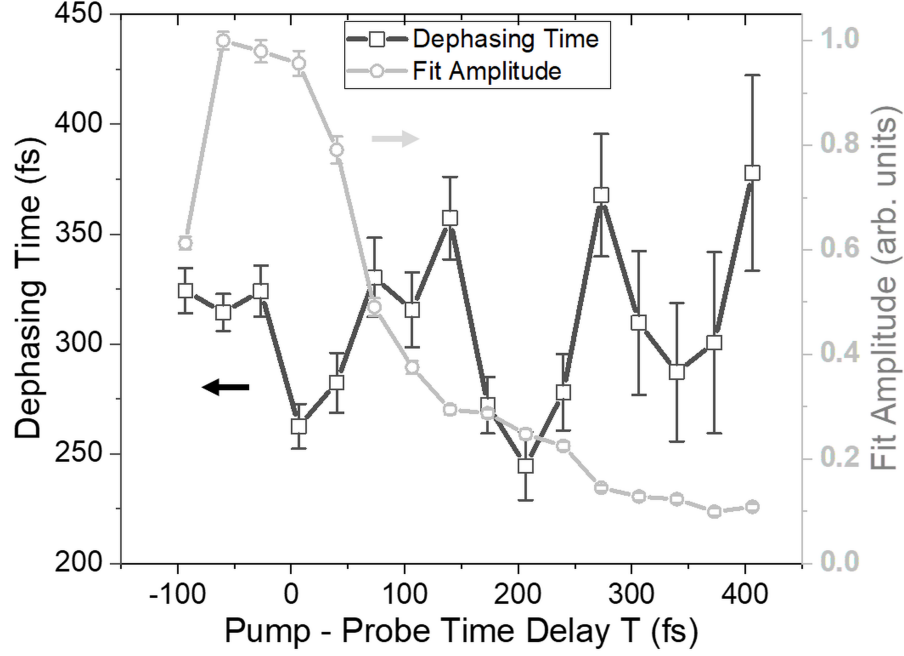


Figure 3: Dephasing times $\gamma(T)$ (black squares and solid black line) for delay scans of the probe pulse and the Kerr gate (τ axis), extracted using the fit of Equation 5, as a function of the pump-probe delay T , for the probe UTPS signal (Figure 2 (a)). Error bars are one standard deviation and become large beyond $T = 250$ fs, as the signal vanishes at larger values of T . $\gamma(T)$ is a measurement of the dephasing time of vibrational coherences on the S_1 excited state and shows oscillations with a period of 177 ± 9.6 fs (see Figure 4 (a)). Grey circles and solid grey line show the fit amplitude $A(T)$ with error bars representing one standard deviation.

$$I_{sig}(\tau; T) = A(T)[H(\tau - t_0(T))\exp(-\frac{\tau - t_0(T)}{\gamma(T)})] \otimes [g(\tau; \sigma)] \quad (5)$$

where $A(T)$ is the amplitude, $H(\tau - t_0(T))$ is the Heaviside step function, $t_0(T)$ is the onset time that quantifies the location of the rise of the signal, $\gamma(T)$ is the decay time of the exponential function, $g(\tau; \sigma)$ is a Gaussian function with width σ , which approximates the instrument response (the cross correlation function of the pulses). See Supporting Information for more details.

The parameter γ as a function of T obtained from the fitting procedure, is plotted in Figure 3 (black squares and solid black line). $\gamma(T)$ is a measure of the dephasing time of the excited state vibrational coherences. The dephasing time is seen to oscillate with a period of 177 ± 9.6 fs (see Figure 4 (a)) as a function of time delay T after excitation of the molecule by the pump pulse. The oscillation amplitude is significantly larger than the error bars that represent one standard-deviation. Figure 3 also shows the fit amplitude $A(T)$ with one standard deviation error bars. The fit amplitude decays and has a weak oscillation which is approximately one half-cycle out of phase with the dephasing time oscillation. As shown in the previous section, the measured signal has contributions from both the ground state and excited state third-order response, even after subtraction of the two ground state-only contributions in Equation 2. However, only the excited state response $\chi_{eff,ex}^{(3)}(\tau, T)$ is dependent on both delay parameters T and τ . Thus the dephasing time $\gamma(T)$, measured for the τ axis as a function of T , should directly correspond to the excited state dynamics of S_1 . On the other hand, $A(T)$ has contributions from both ground and excited states. As a result, the time scale of decay of the amplitude $A(T)$ does not correspond to the excited state lifetime. However, the oscillatory component of $A(T)$, which resembles the dephasing time oscillation, likely corresponds to the excited state dynamics.

The process of Impulsive Stimulated Raman Scattering (ISRS) can compete with two-photon absorption of the pump pulse. Most intramolecular Raman modes in nitrobenzene lie beyond the bandwidth of our pump pulse (~ 80 meV), however a few within the bandwidth are of either weak or moderate strength.³⁰ The relevant moderate strength bands have frequencies at ~ 76 meV (611 cm^{-1}), 49 meV (394 cm^{-1}) and 22 meV (176 cm^{-1}). Since all these modes could be expected to contribute with comparable strength, the time scale of any oscillations observed in the experiment due to ISRS should correspond to beats between these modes. Our measured oscillation period of ~ 177 fs does not correspond to any of these beats, therefore it appears that ISRS does not contribute significantly to the measured signal. Librational excitation on the ground electronic state of nitrobenzene is

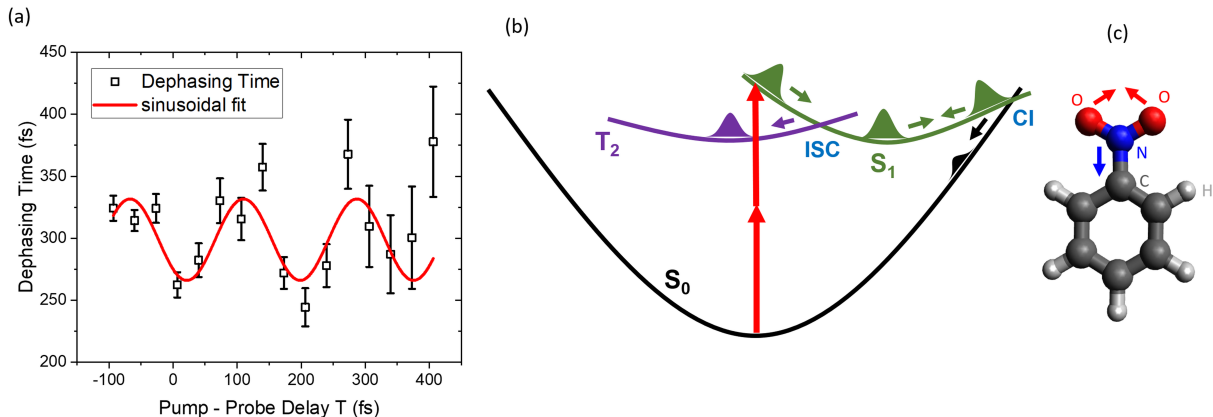


Figure 4: (a) A sinusoidal weighted fit of the dephasing time oscillations seen in figure 3. The fit gives an oscillation period of 177 ± 9.6 fs. (b) Schematic of the different pathways taken by the excited wave-packet based on reference.¹⁸ The wave-packet, excited by two photons from the pump pulse, moves towards the S_1/T_2 inter-system crossing (ISC). A portion of the wave-packet crosses to the T_2 state, and the remaining portion moves towards the S_1/S_0 conical intersection (CI). At the CI a small portion of the wave-packet crosses to the S_0 state, and the remaining portion returns towards the ISC to complete one full period of oscillation. The wave-packet then starts its second oscillation, and by the time it reaches the CI, most of the wave-packet leaves the S_1 state. (c) Structural illustration of nitrobenzene with red and blue arrows indicating O-N-O angle closing and C-N bond shortening, respectively, which are the dominant degrees of freedom as the wave-packet undergoes dynamics on the S_1 state.¹⁸

another possible competing process.³¹ The time scale of librational dephasing, typically >1 ps, is much longer than the dephasing times observed in the present experiments indicating that librational excitation on the ground electronic state does not contribute significantly to the UTPS signal on sub-ps timescales.

Based on recent electronic structure calculations,¹⁸ we propose the following possible explanation for the observed oscillations in $\gamma(T)$. After excitation to the S_1 excited state, the nuclear wave-packet undergoes significant O-N-O angle closing and C-N bond shortening (Figure 4 (c)). As illustrated in Figure 4 (b), the wavepacket moves along the S_1 surface and encounters the ISC region first.¹⁸ The wave-packet then bifurcates to the T_2 state. The remaining portion continues along the S_1 surface, primarily with further C-N shortening to 1.241 Å and O-N-O angle closing to 94.77° , to reach the S_1/S_0 CI, which is elevated by 0.6 eV¹⁷ or 0.3 eV¹⁸ relative to the ISC potential energy. Since coupling between the S_1

Table 1: Geometry-dependence of single molecule $\chi_{eff}^{(3)}$ (arbitrary units) for the S_0 , S_1 , and T_2 electronic states, calculated using the sum-over-states method and density functional theory, with the B3LYP exchange correlation functional. All geometries are from Giussani and Worth.¹⁸

Geometry	S_0	S_1	T_2
S_0 minimum	5.7	123.9	14.3
$S_1(n\pi^*)$ minimum	4.5	8.4	7.5
$T_2(\pi\pi^*)$ minimum	3.7	9.9	8.3
S_1/S_0 CI	7.5	9.0	7.9
S_1/T_2 ISC	4.5	8.3	7.2

and S_0 CI is small,¹⁸ only a small fraction continues onto the S_0 surface. The remaining wave-packet migrates toward the ISC region a second time at $T \approx 200$ fs. The small signal observed in Figure 2 (a) and increasing error bars for the dephasing time (Figure 3) at $T \approx 300$ fs are consistent with a small portion of the wave-packet remaining on the S_1 surface. This suggests that the wave-packet encounters the ISC region three times before the excited-state population completely leaves the initially excited S_1 state by oscillating between the ISC and CI regions along the potential energy surface (Figure 4 (b)).

This picture is supported by our theoretical calculations of $\chi_{eff}^{(3)}$ in the ground and excited states, which are summarized in Table 1. From the calculations we expect the signal to be dominated by $\chi_{eff,ex}^{(3)}$, which is larger for the S_1 state in the Franck-Condon region, specifically at the S_0 minimum geometry, compared with the S_0 and T_2 contributions, which are smaller by an order of magnitude or more. Likewise, S_1 contributions to $\chi_{eff}^{(3)}$ decrease markedly in geometries away from the Frank-Condon region. Therefore, as the wave-packet evolves along the S_1 surface, the $\chi_{eff}^{(3)}$ signal is lost due to (i) nonadiabatic transitions to the S_0 and T_2 states, and (ii) nuclear wavepacket motion away from the Franck-Condon region.

Conclusions

In conclusion, we have demonstrated that ultrafast time-resolved measurements of the third-order nonlinear response of a photoexcited liquid is sensitive to nonadiabatic transitions

between excited electronic states, providing information that can be used to track ultrafast molecular dynamics. Using the optical Kerr effect along with a pump pulse in the Ultrafast Transient Polarization Spectroscopy scheme can offer significant advantages. The dephasing time of vibrational coherences on the excited S_1 state oscillates as a function of the time delay after pump excitation. This variation in dephasing time indicates oscillatory behavior of the excited wave-packet. We find that three encounters of the ISC region by the wave-packet are necessary for the population to completely leave the S_1 surface. The approach of UTPS has the potential for sensitively probing wave-packet dynamics near CIs in molecules, and the simple optical instrumentation is compatible with applications involving a wide range of photon energies, including extreme-ultraviolet and soft X-rays. Future experimental developments could combine third-order response measurements by UTPS with transient absorption spectroscopy, to measure binding energies and electronic character of the states involved, allowing ultrafast transient features to be revealed within congested spectra.

Supporting Information

Supporting Information contains details about the curve fitting analysis of the UTPS data.

Acknowledgement

This work was supported by the U.S. Department of Energy, Office of Science, Office of Basic Energy Sciences, Chemical Sciences, Geosciences, and Biosciences Division. Work at the Molecular Foundry was supported by the Office of Science, Office of Basic Energy Sciences, of the U.S. Department of Energy under Contract No. DE-AC02-05CH11231. This research used resources of the National Energy Research Scientific Computing Center, a DOE Office of Science User Facility supported by the Office of Science of the U.S. Department of Energy under Contract No. DE-AC02-05CH11231.

References

- (1) Worth, G. A.; Cederbaum, L. S. Beyond Born-Oppenheimer: Molecular Dynamics Through a Conical Intersection. *Annu. Rev. Phys. Chem.* **2004**, *55*, 127–158.
- (2) Champenois, E. G.; Shivaram, N. H.; Wright, T. W.; Yang, C.-S.; Belkacem, A.; Cryan, J. P. Involvement of a Low-Lying Rydberg State in the Ultrafast Relaxation Dynamics of Ethylene. *J. Chem. Phys.* **2016**, *144*, 014303.
- (3) Champenois, E. G.; Greenman, L.; Shivaram, N.; Cryan, J. P.; Larsen, K. A.; Rescigno, T. N.; McCurdy, C. W.; Belkacem, A.; Slaughter, D. S. Ultrafast Photodissociation Dynamics and Nonadiabatic Coupling Between Excited Electronic States of Methanol Probed by Time-Resolved Photoelectron Spectroscopy. *J. Chem. Phys.* **2019**, *150*, 114301.
- (4) Timmers, H.; Zhu, X.; Li, Z.; Kobayashi, Y.; Sabbar, M.; Hollstein, M.; Reduzzi, M.; Martínez, T. J.; Neumark, D. M.; Leone, S. R. Disentangling Conical Intersection and Coherent Molecular Dynamics in Methyl Bromide with Attosecond Transient Absorption Spectroscopy. *Nat. Commun.* **2019**, *10*.
- (5) Buckup, T.; Kraack, J. P.; Marek, M. S.; Motzkus, M. In *Ultrafast Phenomena in Molecular Sciences*; de Nalda, R., Bañares, L., Eds.; Springer International Publishing: Cham, 2014; Vol. 107; pp 205–230.
- (6) Ding, F.; Van Kuiken, B. E.; Eichinger, B. E.; Li, X. An Efficient Method for Calculating Dynamical Hyperpolarizabilities Using Real-Time Time-Dependent Density Functional Theory. *J. Chem. Phys.* **2013**, *138*, 064104.
- (7) Marroux, H. J. B.; Fidler, A. P.; Neumark, D. M.; Leone, S. R. Multidimensional Spectroscopy with Attosecond Extreme Ultraviolet and Shaped Near-Infrared Pulses. *Sci. Adv.* **2018**, *4*, eaau3783.

- (8) McMorro, D.; Lotshaw, W.; Kenney-Wallace, G. Femtosecond Optical Kerr Studies on the Origin of the Nonlinear Responses in Simple Liquids. *IEEE J. Quantum Electron.* **Feb./1988**, *24*, 443–454.
- (9) Palese, S.; Schilling, L.; Miller, R. J. D.; Staver, P. R.; Lotshaw, W. T. Femtosecond Optical Kerr Effect Studies of Water. *J. Phys. Chem.* **1994**, *98*, 6308–6316.
- (10) Zhu, X.; Farrer, R. A.; Fourkas, J. T. Optical Kerr Effect Spectroscopy Using Time-Delayed Pairs of Pump Pulses with Orthogonal Polarizations. *J. Phys. Chem. B* **2005**, *109*, 8481–8488.
- (11) Hause, M. L.; Herath, N.; Zhu, R.; Lin, M. C.; Suits, A. G. Roaming-Mediated Isomerization in the Photodissociation of Nitrobenzene. *Nat. Chem.* **2011**, *3*, 932–937.
- (12) Blackshaw, K. J.; Ortega, B. I.; Quartey, N.-K.; Fritzeen, W. E.; Korb, R. T.; Ajmani, A. K.; Montgomery, L.; Marracci, M.; Vanegas, G. G.; Galvan, J. et al. Non-statistical Dissociation Dynamics of Nitroaromatic Chromophores. *J. Phys. Chem. A* **2019**, *123*, 4262–4273.
- (13) Takezaki, M.; Hirota, N.; Terazima, M. Relaxation of Nitrobenzene from the Excited Singlet State. *J. Chem. Phys.* **1998**, *108*, 4685–4686.
- (14) Schalk, O.; Townsend, D.; Wolf, T. J.; Holland, D. M.; Boguslavskiy, A. E.; Szöri, M.; Stolow, A. Time-Resolved Photoelectron Spectroscopy of Nitrobenzene and Its Aldehydes. *Chem. Phys. Lett.* **2018**, *691*, 379–387.
- (15) Xu, S.; Lin, M. C. Computational Study on the Kinetics and Mechanism for the Unimolecular Decomposition of $\text{C}_6\text{H}_5\text{NO}_2$ and the Related $\text{C}_6\text{H}_5 + \text{NO}_2$ and $\text{C}_6\text{H}_5\text{O} + \text{NO}$ Reactions. *J. Phys. Chem. B* **2005**, *109*, 8367–8373.
- (16) Takezaki, M.; Hirota, N.; Terazima, M.; Sato, H.; Nakajima, T.; Kato, S. Geometries

- and Energies of Nitrobenzene Studied by CAS-SCF Calculations. *J. Phys. Chem. A* **1997**, *101*, 5190–5195.
- (17) Mewes, J.-M.; Jovanović, V.; Marian, C. M.; Dreuw, A. On the Molecular Mechanism of Non-Radiative Decay of Nitrobenzene and the Unforeseen Challenges This Simple Molecule Holds for Electronic Structure Theory. *Phys Chem Chem Phys* **2014**, *16*, 12393–12406.
- (18) Giussani, A.; Worth, G. A. Insights into the Complex Photophysics and Photochemistry of the Simplest Nitroaromatic Compound: A CASPT2//CASSCF Study on Nitrobenzene. *J. Chem. Theory Comput.* **2017**, *13*, 2777–2788.
- (19) Takezaki, M.; Hirota, N.; Terazima, M. Nonradiative Relaxation Processes and Electronically Excited States of Nitrobenzene Studied by Picosecond Time-Resolved Transient Grating Method. *J. Phys. Chem. A* **1997**, *101*, 3443–3448.
- (20) Marek, M. S.; Buckup, T.; Motzkus, M. Direct Observation of a Dark State in Lycopene Using Pump-DFWM. *J. Phys. Chem. B* **2011**, *115*, 8328–8337.
- (21) Lotshaw, W. T.; McMorro, D.; Thant, N.; Melinger, J. S.; Kitchenham, R. Intermolecular Vibrational Coherence in Molecular Liquids. *J. Raman Spectrosc.* **1995**, *26*, 571–583.
- (22) Park, S.; Kim, J.; Scherer, N. F. Two-Dimensional Measurements of the Solvent Structural Relaxation Dynamics in Dipolar Solvation. *Phys. Chem. Chem. Phys.* **2012**, *14*, 8116.
- (23) Underwood, D. F.; Blank, D. A. Measuring the Change in the Intermolecular Raman Spectrum during Dipolar Solvation. *J. Phys. Chem. A* **2005**, *109*, 3295–3306.
- (24) Nakano, M.; Yamaguchi, K. A Proposal of New Organic Third-Order Nonlinear Optical

- Compounds. Centrosymmetric Systems with Large Negative Third-Order Hyperpolarizabilities. *Chem. Phys. Lett.* **1993**, *206*, 285–292.
- (25) Pierce, B. M. A Theoretical Analysis of Third-Order Nonlinear Optical Properties of Linear Polyenes and Benzene. *J. Chem. Phys.* **1989**, *91*, 791–811.
- (26) Giannozzi, P.; Baroni, S.; Bonini, N.; Calandra, M.; Car, R.; Cavazzoni, C.; Ceresoli, D.; Chiarotti, G. L.; Cococcioni, M.; Dabo, I. et al. Quantum Espresso: A Modular and Open-Source Software Project for Quantum Simulations of Materials. *J. Phys.: Condens. Matter* **2009**, *21*, 395502.
- (27) Dickson, T. R. Time-Resolved Optical Kerr Effect Spectroscopy by Four-Wave Mixing. Ph.D. thesis, University Of Toronto (Canada)., 1991.
- (28) Kwak, C. H.; Kim, G. Y. Rigorous Theory of Molecular Orientational Nonlinear Optics. *AIP Advances* **2015**, *5*, 017124.
- (29) Vidal, B.; Murrell, J. N. The Effect of Solvent on the Position of the First Absorption Band of Nitrobenzene. *Chemical Physics Letters* **1975**, *31*, 46–47.
- (30) Khaikin, L. S.; Kochikov, I. V.; Grikin, O. E.; Tikhonov, D. S.; Baskir, E. G. IR Spectra of Nitrobenzene and Nitrobenzene-15N in the Gas Phase, Ab Initio Analysis of Vibrational Spectra and Reliable Force Fields of Nitrobenzene and 1,3,5-Trinitrobenzene. Investigation of Equilibrium Geometry and Internal Rotation in These Simplest Aromatic Nitro Compounds with One and Three Rotors by Means of Electron Diffraction, Spectroscopic, and Quantum Chemistry Data. *Structural Chemistry* **2015**, *26*, 1651–1687.
- (31) Smith, N. A.; Meech, S. R. Ultrafast Dynamics of Polar Monosubstituted Benzene Liquids Studied by the Femtosecond Optical Kerr Effect. *The Journal of Physical Chemistry A* **2000**, *104*, 4223–4235.

TOC Image

